Sensors & Transducers, Vol. 250, Issue 3, March 2021, pp. 10-17

Sensors & Transducers

Published by IFSA Publishing, S. L., 2021
http://www.sensorsportal.com

Pressure Transducer Optimization by Multiphysics Simulation

[1] Ricardo PEREIRA and [2, *] Carlos CIMA

[1] UNISINOS, Avenida Unisinos, 950 – São Leopoldo, 93022-750, Brazil
[2] UNISINOS, Avenida Unisinos, 950 – São Leopoldo, 93022-750, Brazil
[2] Tel.: +55.51.3590-8483, fax: +55.51.3590-8305
E-mail: carloscima@unisinos.br

Received: 23 December 2020 /Accepted: 11 February 2021 /Published: 31 March 2021

Abstract: Pressure sensors are used in a wide range of applications with a significant market share in the industrial sector. The piezoresistive pressure sensor is quite popular due to its low production cost. It is normally made up of sensing elements attached to a deformation membrane. The analysis of the mechanical deformation in the elastic element of the sensors plays a critical role in its design. In this paper, the design of a pressure sensor with semiconductor piezoresistive elements was tested and validated via simulation with the COMSOL software. The emphasis was put on the evaluation of the membrane thermal expansion effect on the overall pressure sensor operation. This observation allowed the conduction of a study to minimize the observed thermal effect. Through the simulation it was also possible to evaluate different arrangements and positioning of the semiconductor sensors in order to obtain the best sensitivity and less non-linearity. The best adhesive for the semiconductor resistors attachment was determined through experimental sensitivity and creeping tests. The complete pressure sensor was then prototyped and fully characterized. The final experimental results confirmed the simulated data and the proposed method for reducing the sensor temperature sensitivity.

Keywords: Pressure sensor, Piezoresistor, Displacement analysis.

1. Introduction

In industrial applications, pressure is one of the most popular variables measured in process control systems. Its widespread usage is mainly due to the relative ease of measurement and versatility. It is also possible to infer other process variables, such as level, volume, flow, and density from the pressure values. Considering their wide range of applications, pressure sensors are routinely submitted to the most diverse working conditions and environments while keeping in compliance with the industry performance and reliability requirements.

The piezoresistance effect in silicon was discovered by C. S. Smith in 1954 [1]. The first piezoresistive semiconductor sensors used in strain measurement were reported in the early 1970s in applications for the automotive industry. Pressure sensors based on silicon piezoresistive devices have been the subject of intense research and used in commercial applications ever since [2]. Its main advantages are the high sensitivity and the high resistance value, as well as the small size.

Currently, pressure sensors based on the phenomenon of piezoresistivity in silicon are widely used not only due to their good performance figures, but also for its low production cost. However, the process of encapsulating these pressure sensors is still delicate [3].

The pressure sensor presented in this work was designed to operate in the industrial environment and its principle of transduction is the piezoresistivity effect in the semiconductor material. The sensor design seeks to create and optimize a low-cost solution. The device uses silicon sensors, but the semiconductor substrate is not directly exposed to the material on which the pressure is exerted. Instead, the sensors are fixed on a stainless steel membrane, which guarantees contact compatibility with a wide range of materials.

Usually, the sensor output signal needs correction and compensation. Some non-linearities and/or influences of other physical quantities, such as temperature, must be corrected for achieving its best performance. Hence, the characterization of the sensor is essential to describe its behavior and evaluate the main factors affecting its operation.

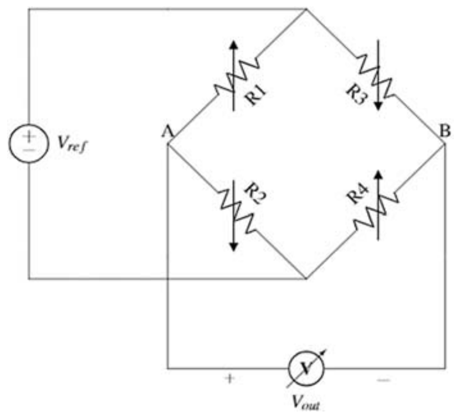

Fig. 1. Full Wheatstone bridge.

2. Piezoresistive Pressure Sensors

Most piezoresistive pressure sensors nowadays are intended for the automotive and healthcare sectors, however, the industrial area also has a relevant market share [4].

The piezoresistive effect is a phenomenon observed in metals and semiconductors, which relates the variation in the electrical resistance of the material with the applied mechanical strain. A useful variable used to quantify the piezoresistive effect is the Gauge Factor (GF), defined as the ratio of the relative change in resistance (R) to the relative change in material length (*l*). The GF value in semiconductor materials can be up to two orders of magnitude higher than that of metals. This high sensitivity allows the use of a lower excitation voltage. It also permits the mechanical structure deformation to remain in a region further away from the point of plastic deformation [5].

In many applications, the piezoresistive pressure sensor consists of two basic elements: a deformation membrane and the piezoresistive deformation sensor [6]. There are many techniques to carry out the sensor construction and manufacture. The most common ones involve fixing the piezoresistors on a membrane which undergoes a tension (stress) proportional to the pressure applied to it. The piezoresistive deformation sensor will change its electrical resistance as a result of the mechanical deformation generated by the pressure.

The piezoresistive deformation sensors must be positioned on the membrane surface taking into account its deformation condition. In addition, the piezoresistors are commonly connected in an electrical configuration based on the Wheatstone bridge. The Wheatstone bridge can be fed either by a current source or by a voltage power supply. There are three basic configurations for the construction of the Wheatstone bridge: quarter bridge, half bridge, and full bridge. Among these possibilities, the full bridge is usually the most widely used, because it provides good pressure response and low sensitivity to temperature variations. Fig. 1 shows the configuration of a full Wheatstone bridge.

3. Pressure Sensor Design and Fabrication

The piezoresistive deformation sensors were manufactured using 6-inch Czochralski-grown silicon (Si) wafer with a thickness of 625 μm and <100> crystalline orientation. Originally, the wafer had a thin native layer of silicon dioxide (SiO_2) on the surface, which was removed during a cleaning step before any processing. The wafer was subsequently oxidized in a diffusion furnace, resulting in a thick layer of high quality silicon dioxide (~850 nm). A polycrystalline silicon (poly-Si) film was then deposited by LPCVD (Low Pressure Chemical Vapor Deposition) on the wafer using phosphorus (P) as the doping element. The resulting poly-Si layer has a uniform ***n***-type doping concentration of 1.05×10^{20} cm^{-3} and a thickness of 450 nm. This layer is the piezoresistive element in the semiconductor structure. After the LPCVD step, the wafer was submitted to a photolithography process, in which the shape of the sensing element is defined by an appropriate mask and the subsequent etching. The aluminum (Al) pads for the poly-Si resistor were deposited by PVD (Physical Vapor Deposition) and defined by another photolithography step and chemical etching. After annealing, the entire wafer was grinded to a desired thickness (70 μm). The final step is the wafer dicing, producing the individual resistors. The strain device has a length of 1 mm and a width of 0.6 mm, as shown in Fig. 2.

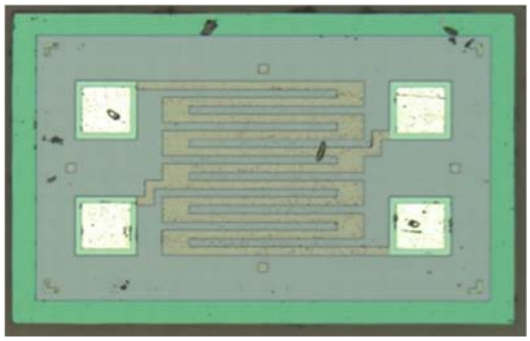

Fig. 2. Piezoresistive strain sensor.

At room temperature, the piezoresistor average resistance is 3.7 kΩ (without being submitted to any deformation) which corresponds to an average sheet resistance (Rs) of 17 Ω/□. According to the working principle of the piezoresistance, the change in resistance, caused by an induced change in the resistivity (Δρ), is related to the stress (σ) by the constitutive relationship presented in Eq. (1), where Π is the piezoresistance tensor (SI units: $Pa^{-1}\cdot\Omega\cdot m$), a material property.

$$\Delta\rho = \Pi\,\sigma \tag{1}$$

The piezoresistive tensor coefficients depend on carrier concentration and operating temperature [7]. In general, the relationship between them is inverse, i.e., the higher the temperature and/or the carrier concentration, the lower is the value of the tensor coefficients, thus decreasing the sensor sensitivity.

The other essential component for the construction of the pressure sensor is the deformation membrane. Several different deformation membrane shapes can be used. The most common shapes are the circular, the rectangular and the square ones. The circular membrane shows the highest deformation under the same applied pressure condition. Additionally, this deformation happens with the lowest level of stress, when compared to the other shapes [8]. However, the square membrane has the highest sensitivity and the best linearity. Considering membranes with the same area, circular and square shapes produce the best performance [9]. Although the square membrane is the one with the highest sensitivity, a circular membrane was chosen to develop the present work, because this shape has a simple construction process with metallic materials. This is aligned with the purpose of developing a low-cost sensor.

The membrane thickness and radius settings have been defined based on the sensor working pressure range. These dimensions were determined in order to obtain a pressure sensor with a working pressure of up to 1 MPa. The working pressure of the sensor is extremely important to design the mechanical system of the pressure sensor. A displacement and stress analysis must be done to check the behavior of the mechanical deformation. The presence of plastic deformation would compromise the proper work of the sensor, since the piezoresistor element would remain submitted to a deformation that is no longer related to the applied pressure. Therefore, the maximum operating pressure to which they could be subject must not exceed the flow limit of the membrane material. In order to determine the maximum pressure the membrane can withstand without exceeding its flow limit, a few factors must be taken into account, such as the shape of the membrane, its material properties, thickness, and surface roughness. In the case of the circular membrane, Eq. (2) defines the maximum pressure (Pb) that can be applied to it, where F_{Max} is the flow limit of the membrane material, A is the area of the diaphragm, h is the thickness of the diaphragm and ν is the Poisson's ratio of the material (supposing the material membrane is ductile) [10].

$$Pb = \frac{3.4F_{Max}h^2}{A(1-\nu^2)} \tag{2}$$

Defining the membrane material as 316 stainless steel, the diameter as 8 mm, and the maximum pressure as 1 MPa, Eq. (2) was used to determine the diaphragm thickness as 220 µm. Fig. 3 shows a deformation membrane with the four piezoresistors placed in initial positions, since their precise location has not yet been defined (the outer diameter is 18 mm).

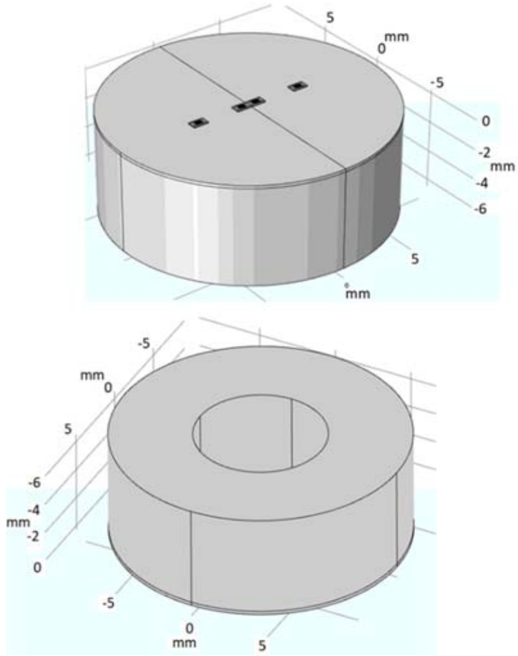

Fig. 3. Deformation membrane (upside and downside views).

The silicon devices must be attached to the membrane with an adhesive that can transmit the deformation of the membrane to the piezoresistor sensors in a reliable way. Therefore, different types of adhesives must be tested to check which one has the best performance. In this context, four adhesives were chosen to be submitted to a test: two epoxy, one cyanoacrylate and one phenolic-based material. For each type of adhesive, 6 piezoresistors were fixed on a 200 µm thick stainless steel cantilever beam. The electrical contact to the sensor terminals was provided by 17 mm-thick gold wires soldered using a wire bonding tool. This structure allowed the measurement of the resistance behavior for each piezoresistor under different deformation conditions. Fig. 4 shows one of the beams with the piezoresistor sensors bonded on its surface.

One of the ends of the beam was fixed, whereas the other end received the application of a mechanical force causing a deformation in the metal sheet. This mechanical strain was created by calibrated masses suspended at the beams' edge. Fig. 5 illustrates the experimental arrangement used in the deformation analysis.

Fig. 4. Piezoresistor elements attached to a cantilever beam using different adhesives.

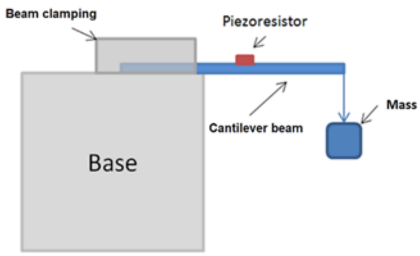

Fig. 5. Experimental arrangement used for the adhesives' testing.

The resistance measurement was done using the Keysight 34401A digital multimeter. For each weight value applied to the beam, a series of 6 measurements was performed. The experiment was carried out applying 7 different weight values: 0, 20, 50, 70, 100, 120, 150 g. Hence, for each adhesive under test, a total of 252 measurements were taken. In the graph shown in Fig. 6, one can view the resistance behavior with the different tested adhesives. Each point plotted in the graph of the figure denotes the average of all measurements taken in the 6 piezoresistors used for the respective combination of adhesive and weight. The phenolic and the cyanoacrylate-based adhesives presented a very similar sensitivity performance (-0.236 and -0.259 Ω/g, respectively), however this is not enough to warrant the choice of the best material for sensor construction.

Another adhesive test was then executed to further evaluate the adhesion performance of the piezoresistor elements on the deformation membrane using the same experimental setup. This additional experiment is called the creeping test, a procedure based on the observation of the piezoresistor resistance variation over a long period of time while keeping the cantilever beam under a constant deformation condition. The numerical value of the creeping parameter is calculated taking the total resistance variation value ($\Delta R = R_{initial} - R_{final}$) and dividing it by the initial resistance value ($Creeping = \Delta R / R_{initial}$). This provides a good tool for evaluating the entire adhesive set performance comprising the adhesive itself, the deformation membrane, and the piezoresistor element. In the creeping experiment, the cantilever beams with the attached piezoresistors were subject to a constant deformation for a full week (168 hours). During this time, the temperature of the samples was kept constant and resistance measurements were periodically taken. For each tested adhesive, a total of six piezoresistors were again attached to the membrane, thus minimizing the effects of possible construction variations on the final results. The graph in Fig. 7 shows the average resistance of the piezoresistors throughout the creeping test for different adhesives. The best calculated creeping values were shown by the phenolic and the cyanoacrylate-based adhesives (72 and 130 ppm, respectively). In view of these results, the phenolic adhesive was chosen to build the final sensor prototypes.

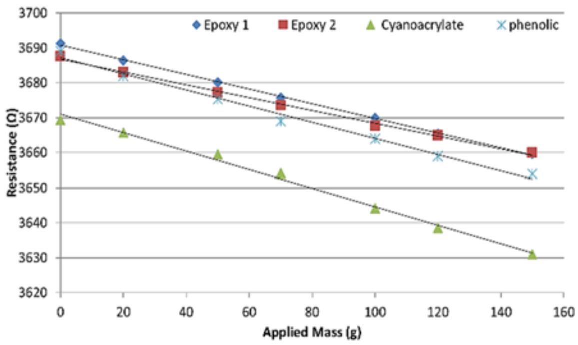

Fig. 6. Experimental resistance variation using different adhesives.

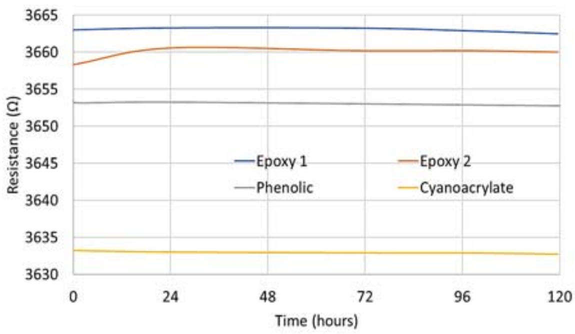

Fig. 7. Piezoresistors resistance during the creeping test.

Before building the transducer, the positioning of the semiconductor sensors on the membrane must be defined through a deformation study of the metallic membrane. The purpose of the analysis is to position the sensor elements at the points where the highest tensile and compression deformation intensities occur. The study was carried out using the physical simulation software COMSOL. For a better performance of the Wheatstone bridge, two of the piezoresistors must be positioned in places where the compression effort occurs and the other two where there is a traction effort. In the circular membrane, the radial and axial stresses on its surface have the same intensity when equidistant from its central point. The points of the same radius, therefore, measured from the center of the membrane, are submitted to the same strain. During the simulations with the COMSOL software, it was possible to verify the behavior of the stress generated by the deformation along the membrane. This allowed the optimization of the piezoresistor positioning on its surface. The graph in Fig. 8 shows the distribution of the mechanical stress alongside the radius of the deformation membrane for a wide range of pressure values. The regions with the highest stress values are indicated in the figure (center and edges).

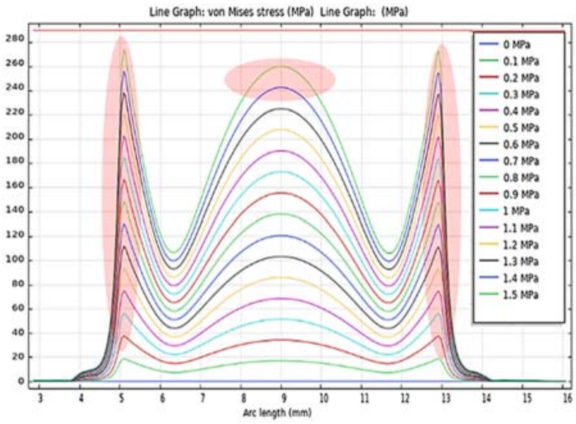

Fig. 8. Distribution of the mechanical stress along the radius of the deformation membrane (simulation).

In addition to the sensitivity, the positioning of the semiconductor sensors on the membrane can also affect its linearity. Another study was then carried out to evaluate the response of the pressure sensor as a function of the different positions where the strain sensors are fixed on the membrane. Distinct arrangements and positions of the strain sensors were simulated, and, in turn, their responses were evaluated. During the simulation, the pressure was varied from 0 MPa to 1 MPa. Fig. 9 shows the proposed positioning arrangements.

For each arrangement shown in Fig. 9, a simulation was done in which the sensor's output signal was checked for different pressure values. During the simulation, the Wheatstone bridge was excited with a current of 2 mA and the measurement of the differential voltage occurred between the intermediate terminals of the Wheatstone bridge. The graph in Fig. 10 shows the output voltage for each position arrangement as a function of the applied pressure.

As is clearly shown in Fig. 10 the arrangement that produces the best sensitivity to the applied pressure is the one identified as Position 1 in Fig. 9. In addition, this arrangement has the smallest non-linearity in its response, as indicated by the graph shown in Fig. 11. Therefore, this arrangement model was chosen for the construction of the pressure transducer.

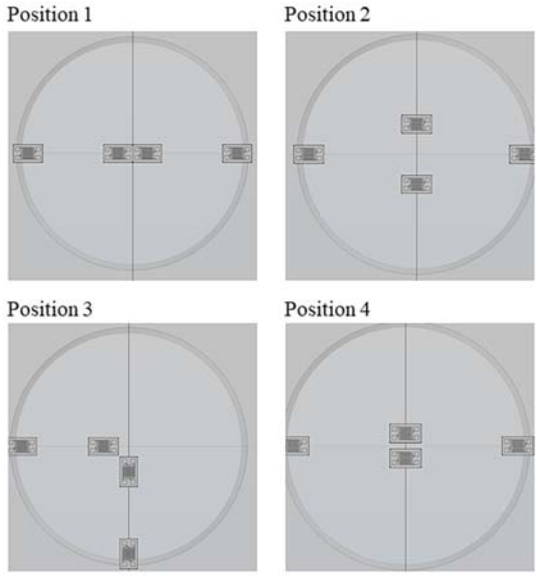

Fig. 9. Proposed arrangements and positions of the strain sensors on the membrane.

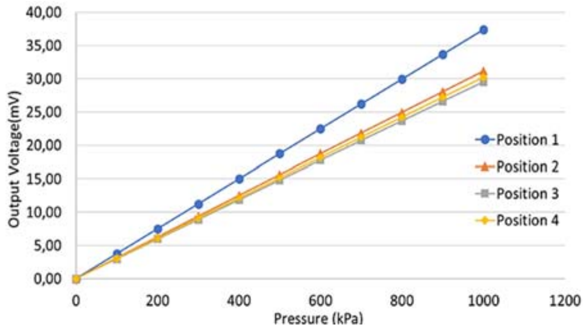

Fig. 10. Sensor output signal for each tested position arrangement (simulation).

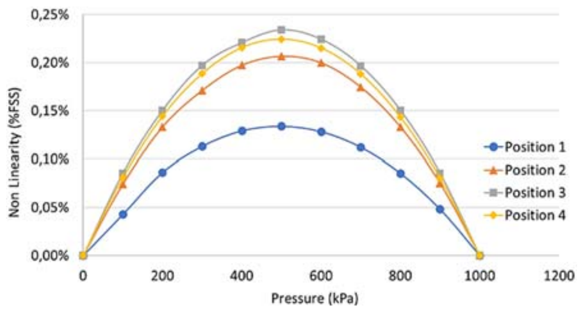

Fig. 11. Non-Linearity of the sensor output signal for each position (simulation).

The simulation of the pressure transducer was also done for different environmental conditions. Keeping the piezoresistors attached to the membrane interconnected in a Wheatstone bridge excited with a constant current of 2 mA, the simulation checked the temperature effect on the overall sensor performance. In this case, the temperature was varied from 0 °C to 100 °C, with the same pressure range of the previous simulations. A combination of simulations was then carried out under these new conditions in order to validate the sensor's operation in a comprehensive way. Fig. 12 shows the output signal generated by bridge for the simulated temperatures and pressures (using the sensors in Position 1).

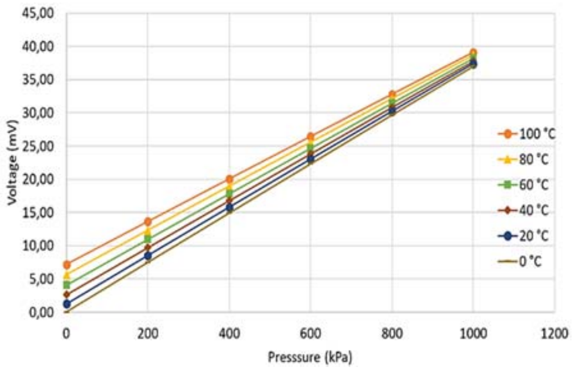

Fig. 12. Simulated output signal from the transducer for different temperatures and relative pressures.

Observing the transducer response curve (Fig. 12), it is evident that the pressure sensor sensitivity is greatly influenced by the temperature. This happens because the temperature affects both the physical properties of the deformation membrane and the semiconductor piezoresistance (which decreases with the temperature variation). It is worth noting that the highest variation in the transducer output voltage (under the same pressure) occurs when there is no pressure applied to the sensor. This represents a significant variation in the sensor offset. In order to determine the cause of this effect, the thermal expansion of the metallic membrane due to the temperature variation was also simulated. The graph in Fig. 13 shows the deformation caused by the membrane thermal expansion alongside the cross section passing through its center under two different temperatures (0 and 100 °C). The value for the partial derivative of the deformation caused by the thermal expansion in relation to the position of the cutting axis under analysis is plotted too.

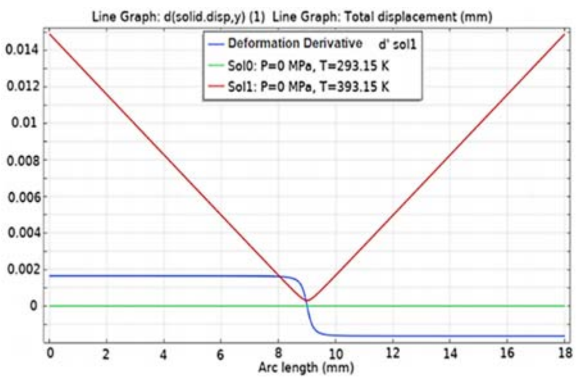

Fig. 13. Deformation caused by the membrane thermal expansion alongside a cross section through its center (simulation).

It is possible to observe that the change rate modulus for thermal expansion is constant in almost all the membrane surface. However, there is a central region in which the thermal expansion does not have a linear behavior. This region coincides with the location where two of the bridge's piezoresistors are positioned. It was expected that these thermal expansion effect would be minimized, since the sensors would be experiencing an expansion of the same intensity, being cancelled by the Wheatstone bridge. The simulation revealed this is not observed, since the central piezoresistors do not experience the same deformation due to the thermal expansion as compared to the piezoresistors at the edge of the membrane, causing a bridge imbalance generated by the temperature variation. In order to minimize this effect, the central region piezoresistors were repositioned so that they remain entirely in the area where the thermal expansion change rate is constant and of the same intensity as in the other piezoresistors. This was accomplished by moving each central piezoresistor 200 μm to the edge of the membrane. Fig. 14 shows the sensor response to different pressures and temperatures after adjusting the position of the central piezoresistors. One notes that there was a significant reduction in the offset of the transducer output signal. In the original arrangement, when the working temperature was changed by 100 °C, the offset voltage changed by 7.2 mV. After changing the position of the piezoresistors, the offset variation was reduced to 0.45 mV.

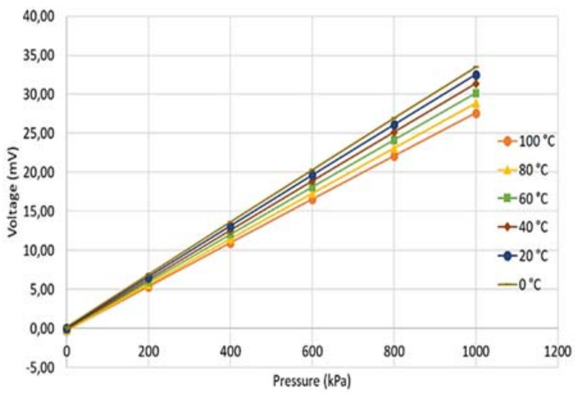

Fig. 14. Transducer output signal for different temperatures and relative pressures after the sensor repositioning (simulation).

After the optimization of the sensor design by simulation, the devices were built and submitted to a set of tests for the characterization. The sensors were subjected to different pressures using a laboratory infrastructure composed of a pressure controller in an environment with controlled climatic conditions. Then the sensors' response was measured under different pressure values. Intermediate pressure values always correspond to a multiple of 20 % of the sensors' full scale. Hence, the pressure was varied from 0 to 1 MPa with an interval of 0.2 MPa between each measurement. Notice that the pressure values used to describe the experiments and the results refer to a relative pressure (with the atmospheric pressure as zero reference). The measurements were carried out by increasing and subsequently decreasing the pressure values applied to the sensor. In addition to checking the pressure applied to the sensor, the sensors' working temperature was controlled and monitored during the tests. Therefore, the sensors' response tests were performed at several temperatures, ranging from 0 to 100 °C. Fig. 15 shows the diagram of the laboratory infrastructure built to perform the tests.

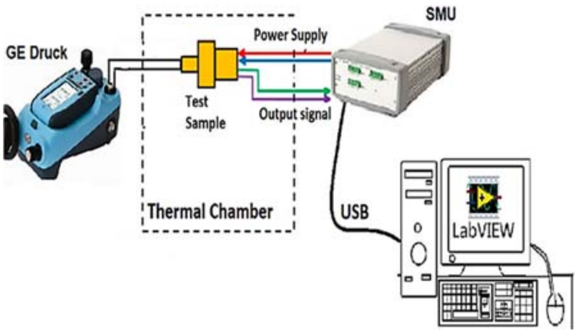

Fig. 15. Laboratory infrastructure diagram.

The measurement data was acquired using an Agilent U2733A SMU (Source Measurement Unit), which makes it possible to automate the experiments using LabView. Therefore, a program was developed using the LabView software, which communicates with the SMU, acquiring the measured data and showing it in the measurement environment. The SMU is responsible for supplying the Wheatstone bridge with the desired current, as well as for measuring the differential voltage of the bridge. The data is acquired for each pressure and temperature condition. A quantity of eight measurements is taken at five-second intervals for each point. Fig. 16 presents the actual laboratory infrastructure used to perform the tests.

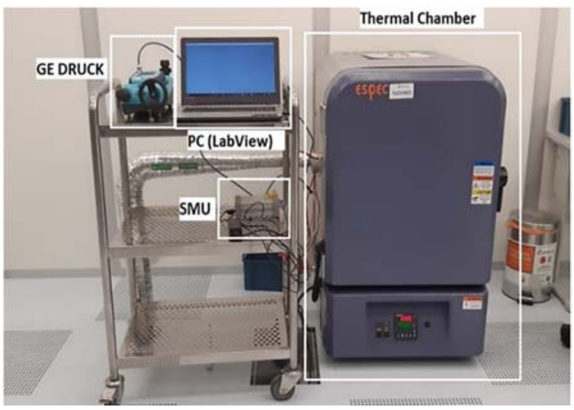

Fig. 16. Laboratory infrastructure used to perform the tests.

In order to check the reduction of the offset variation in a practical way, an experimental test was carried out using three samples for each of the two different positions. In this case, no pressure was applied to the sensor, only the working temperature was changed. During the test, the differential voltage of the Wheatstone bridge was monitored, generating a graph that shows the variation of the sensors' offset voltage for different working temperatures. As can be seen in Fig. 17, the experiment proved the result obtained in the simulation environment. The change in the position of the central sensors resulted in the reduction of the offset variation caused by the temperature.

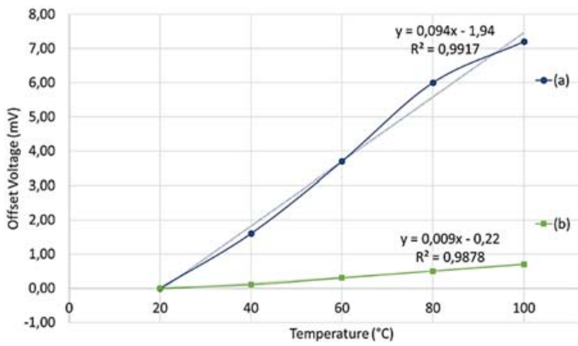

Fig. 17. Experimental variation of the sensors' offset voltage for different working temperatures (no pressure applied): (a) Original position; (b) After repositioning.

After the tests performed to verify how the temperature affects the pressure sensor, experimental measurements with real pressure applied to the sensors were also realized. These tests were performed using pressures ranging from 0 to 1 MPa, and then observing the differential voltage of the Wheatstone bridge. The temperature was varied from 0 to 100 °C for each pressure experiment. Fig. 18 shows the experimental measurements obtained (with the position of the central piezoresistors already corrected). The vertical axis shows the signal of the output voltage with the discount of the offset value at 0 MPa, i. e., only the variation of the output voltage is shown in order to facilitate the visualization of the graphs.

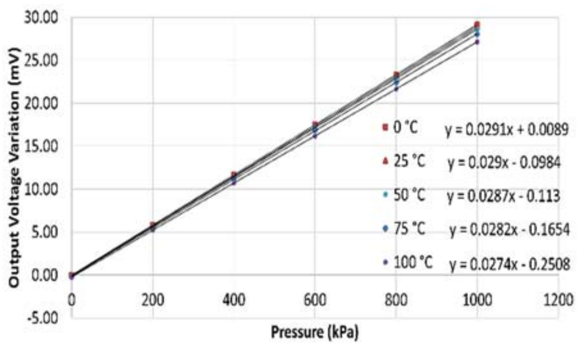

Fig. 18. Experimental output voltage variation under different pressures and temperatures applied to the sensor.

As can be seen in the results obtained during the experimental tests, the sensors show a linear behavior regarding applied pressure. The average variation of the sensors' output voltage, considering the full pressure range, is 29.107 mV. The variation of the offset voltage remained low (0.26 mV) as expected after the sensor repositioning. Conversely, the sensor output signal temperature dependence is still visible, but now it is mostly related to the semiconductor material properties.

When one compares the simulation and the practical results, it is clear that both show the same behavior under the influence of the temperature variation. As the temperature is raised, the sensitivity of the sensor deteriorates, i. e., higher temperatures make the sensor less sensitive to pressure variation. This happens because the temperature reduces the values of the piezoresistance tensor coefficients, resulting in a smaller resistance variation caused by a specific pressure difference.

4. Conclusions

The simulations carried out in the COMSOL software, covering different pressure and temperature conditions, characterized the behavior of a pressure sensor. The analysis of the simulation results was important to validate the sensor operation principle, as well as to evaluate the influence of different physical phenomena on its performance. In particular, the simulation revealed the critical importance of the metal membrane thermal expansion and the sensor positioning for the transducer offset value at zero pressure.

The adhesive used to attach the piezoresistors to the membrane was chosen by an experimental procedure. After the complete simulation of the transducer, prototypes were built in order to check its real behavior. The transducers showed good linearity and low thermal offset variation in the experimental tests, confirming the effectiveness of the piezoresistors repositioning optimization. The interaction between experimental and simulated data proved to be a fast and reliable strategy to optimize the sensor design and fabrication.

Acknowledgements

The authors wish to thank the company Ceitec S. A. for manufacturing the silicon sensing elements used in this work.

References

[1]. Smith C. S., Piezoresistance Effect in Germanium and Silicon, *Physical Review*, Vol. 94, Issue 1, 1954, pp. 42-49.

[2]. Ham S., *et al*., Design, fabrication, and characterization of piezoresisitve strain gage-based pressure sensors for mechatronic systems, in *Proceedings of the IEEE International Workshop of Electronics, Control, Measurement, Signals and their Application to Mechatronics (ECMSM'2015)*, 2015, pp. 3–7.

[3]. Birkelund Karen, *et al*., High-pressure silicon sensor with low-cost packaging, *Sensors and Actuators A: Physical*, Vol. 92, Issue 1-3, 2001, pp. 16-22.

[4]. H. Ngo, *et al*., The roadmap for development of piezoresistive micro mechanical sensors for harsh environment applications, in *Proceedings of the Eleventh International Conference on Sensing Technology (ICST)*, Sydney, NSW, 2017, pp. 1-6.

[5]. Barlian A. A., *et al*., Review: Semiconductor piezoresistance for microsystems, in *Proceedings of the IEEE*, Vol. 97, Issue 3, 2009, pp. 513–552.

[6]. Gustav Gautschi, Pressure Sensors, in Piezoelectric Sensorics, 1st edition, *Berlin: Springer-Verlag*, 2002, pp. 141-165.

[7]. Richter J., *et al*., Piezoresistance in ***p***-type silicon revisited, *Journal of Applied Physics*, Vol. 104, 2008, pp. 023715 - 023715-8.

[8]. Lin Liwei, Chu Huey-Chi, Lu Yen-Wen, A simulation program for the sensitivity and linearity of piezoresistive pressure sensors, *Journal of Microelectromechanical Systems*, Vol. 8, Issue 4, 1999, pp. 514-522.

[9]. Maflin Shaby S., Design and analysis of silicon diaphragm of a MEMS pressure sensor, *ARPN Journal of Engineering and Applied Sciences*, Vol. 10, Issue 5, 2015, pp. 2132-2135.

[10]. Meti Shwetha, Kirankumar B. Balavald, B. G. Sheeparmatti, MEMS piezoresistive pressure sensor: a survey, *International Journal of Engineering Research and Applications*, Vol. 6, Issue 4, part 1, 2016, pp. 23-31.